THE 14TH INTERNATIONAL STELLARATOR WORKSHOP

Neoclassical Transport and Radial Electric Fields in TJ-K

K.Rahbarnia, C.Beidler[(1)], F.Greiner, M.Ramisch, U.Stroth
IEAP, University of Kiel, 24098 Kiel, Germany,
[(1)]MPI für Plasmaphysik, EURATOM Association, Greifswald, Germany

Abstract: The neoclassical transport is investigated in the torsatron TJ-K, which is operated with a low-temperature plasma. In the low-collisionality regime neoclassical losses are not intrinsically ambipolar, leading to the formation of a radial electric field which acts on both neoclassical and turbulent transport. This electric field is measured with a combination of Langmuir and emissive probes. The data are compared with the ambipolar electric field calculated with an analytic model [1]. The experimental fields are positive and larger than the calculated ones. Direct losses of the fast electrons might explain this discrepancy.

Introduction: Because of the high diffusion coefficients in the low collisionality regime, Neoclassical transport is an important element of plasmas confined in stellarators. Since the torsatron TJ-K [2] (formerly TJ-I U [3]) is operated with a low-temperature plasma standard diagnostics, such as Langmuir- and Emissive probes, can be applied to measure the plasma potential in the entire plasma volume. TJ-K is an $l = 1$, $m = 6$ torsatron. Minor and major plasma radii are 0.1 and 0.6 m, respectively, and the magnetic field strength is $B \leq 0.3\,\mathrm{T}$ at $\iota \approx 1/3$. Fig. 1 depicts the Fourier spectrum of the magnetic field configuration of TJ-K. It is calculated from

$$B = \sum_{ml} \{CC_{ml}(\rho)\cos(6Mm\varphi)\cos(l\varphi) + SS_{ml}(\rho)\sin(6Mm\varphi)sin(l\varphi)\}\,. \qquad (1)$$

CC_{ml} and SS_{ml} are polynomials in ρ up to third order. The plasma has central densities up to $n_e = 1 \times 10^{18}\,\mathrm{m}^{-3}$ and electron temperatures up to $T_e = 15\,\mathrm{eV}$. The ions are cold ($< 1\,\mathrm{eV}$). Working gases are Hydrogen, Helium and Argon. For the experiments presented here, the plasma was created by ECRH with a radiated power between 0,6 kW and 1,8 kW. One to the ECRH frequency of 2,45 GHz, the magnetic field was fixed at B $\approx 0,1$ T. A further control parameter is the neutral gas pressure P_0, typically 2×10^{-5}–5×10^{-5} mbar. The discharge duration is up to 60 min.

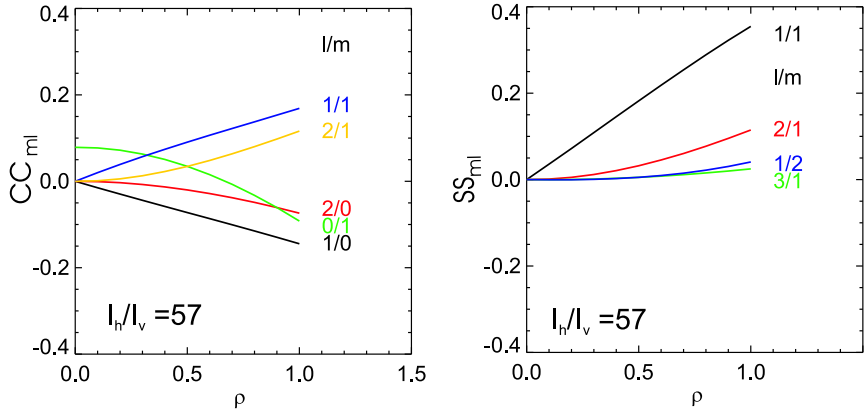

Fig. 1: Fourier coefficients for TJ-K.

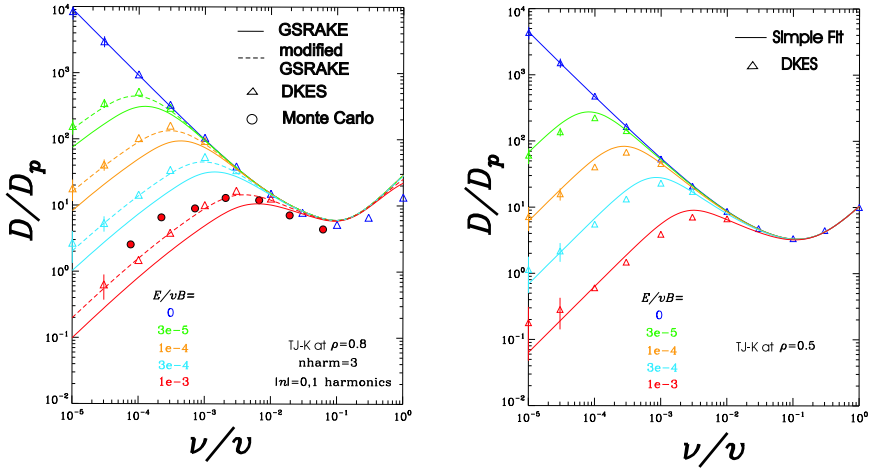

Fig. 2: Mono-energetic diffusion coefficients for TJ-K as a function of the collisionality. left: Solution of some different codes solving the drift kinetic equation at a normalized radius $\rho = 0.8$. right: Adaptation from an easier analytic model to DKES-code at a normalized radius $\rho = 0.5$. All for different electric fields.

Theory and numerical simulation: The neoclassical electric field has to be determined from the ambipolarity between radial electron and ion fluxes $\Gamma_e(r, E_r^{amb}) = \Gamma_i(r, E_r^{amb})$. The fluxes can be calculated from the distribution function

$$\Gamma \sim \int v f(v) \mathrm{d}^3 v \frac{\mathrm{d}r}{\mathrm{d}t}\,, \tag{2}$$

which follows from the drift kinetic equation. The standard procedure [6] is to linearize the equation and carry out the flux surface averaging. For a simple geometry [1] you get the following expression for the particle fluxes:

$$\Gamma = -4\pi\sqrt{\frac{2}{m^3}} \int_0^\infty \sqrt{\kappa} D(\kappa) \frac{\mathrm{d}f_M}{\mathrm{d}r}\,\mathrm{d}\kappa\,, \tag{3}$$

where D is the mono-energetic diffusion coefficient, which only depends on the collision frequency ν and the particle kinetic energy κ. f_M is the Maxwell distribution with the derivative taken at fixed total particle energy

$$\kappa + eU = const. \tag{4}$$

Since the magnetic field configuration of TJ-K (see Fig. 1) is dominated by m = 1 and m = 2 terms, an analytic Anstaz similar to the one of Shaing [1] is reasonable. The analytic forms of the diffusion coefficients were fitted to results from numerical solutions of the DKE. The resulting fits, with an effective ripple increasing from 0,2 to 0,9 from the center to the edge, can be seen in Fig. 2. Here some different solutions for the drift kinetic equation are shown. The left side compares results from GSRAKE (**G**eneral **S**olution of the **R**ipple-**A**veraged **K**inetic **E**quation) [4], a Monte-Carlo-Simulation, which gives reliable results for low collisionalities, and the DKES-code (**D**rift **K**inetic **E**quation **S**olver) [5,7]. The mono-energetic diffusion coefficients are all normalized to the plateau value of the equivalent tokamak with circular flux surfaces

$$D_P = \frac{\pi}{4} \frac{R v_d^2}{\iota v}\,, \tag{5}$$

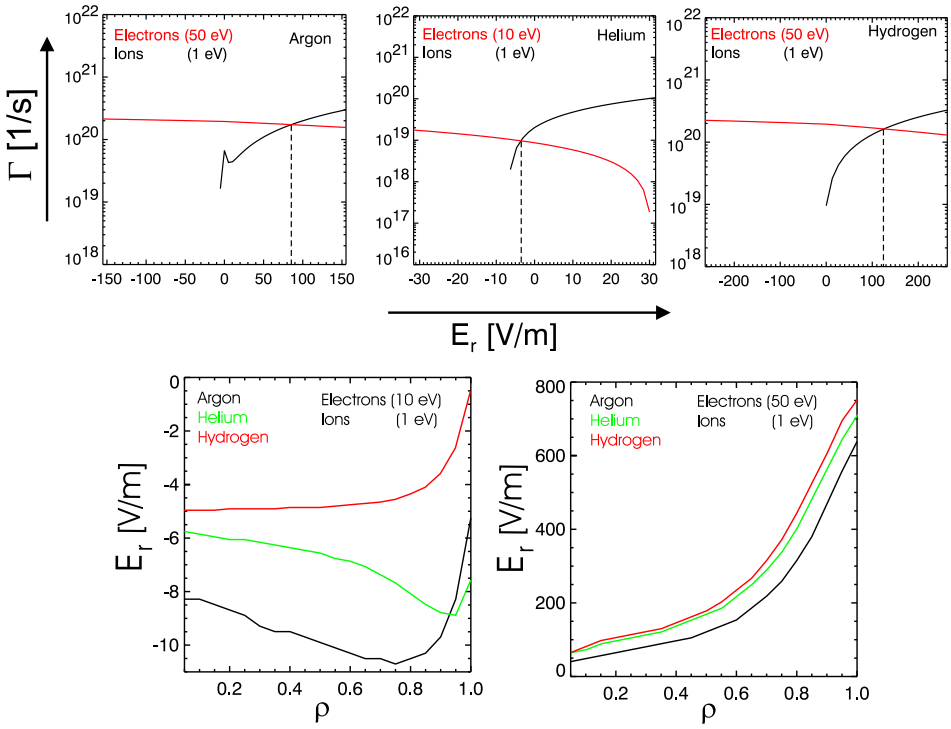

Fig. 3: Top: Electron (red) and ion (black) fluxes as a function of the radial electric field for different plasma parameters. Bottom: Radial profiles of the radial electric field for different ion masses and two sets of plasma parameters with B = 0,9 T.

with v_d the magnitude of the radial drift velocity and v the mono-energetic velocity. The complete mono-energetic diffusion coefficient is given as a sum of three terms: the AXIsymmetric contribution, the Long-Mean-Free-Path portion and an ADDitional term which is needed to describe the transition from the axisymmetric to the $1/\nu$ regime

$$D^* = D^*_{axi} + D^*_{lmfp} + D^*_{add}\,. \tag{6}$$

The * marks the normalization. From the diffusion coefficients and (3) the electron and ion fluxes are calculated. The upper part of Fig. 3 shows examples for plasma parameters in the range of a low-temperature plasma.

For the calculations B = 0,1 T and a density of $1 \cdot 10^{18}\,\mathrm{m}^{-3}$ were assumed. The fluxes are calculated at a normalized plasma radius of $\rho = 0,3$. For lower electron temperatures (10 eV) the ambipolar electric field, which is determined by the intersection of electron and ion fluxes is negative. For higher electron temperatures (up to 50 eV) the diffusion coefficient in the $1/\nu$-regime rises and with this also the particle transport Γ. Because of the high electron losses the plasma charges up positive. The peak at $E_r = 0$ in the ion transport for the gas Argon is due to losses of the helically trapped particles. The bottom part of Fig. 3 illustrates the radial electric field which ensures ambipolarity as a function of the normalized radius ρ. These profiles are compared with experimental results in the next section.

Experimental results: A combination of Langmuir and emissive probes were used to measure radial profiles of the electric potential, electron temperatures and densities for the accessible range of plasma parameters. In Fig. 4 the electron temperatures and

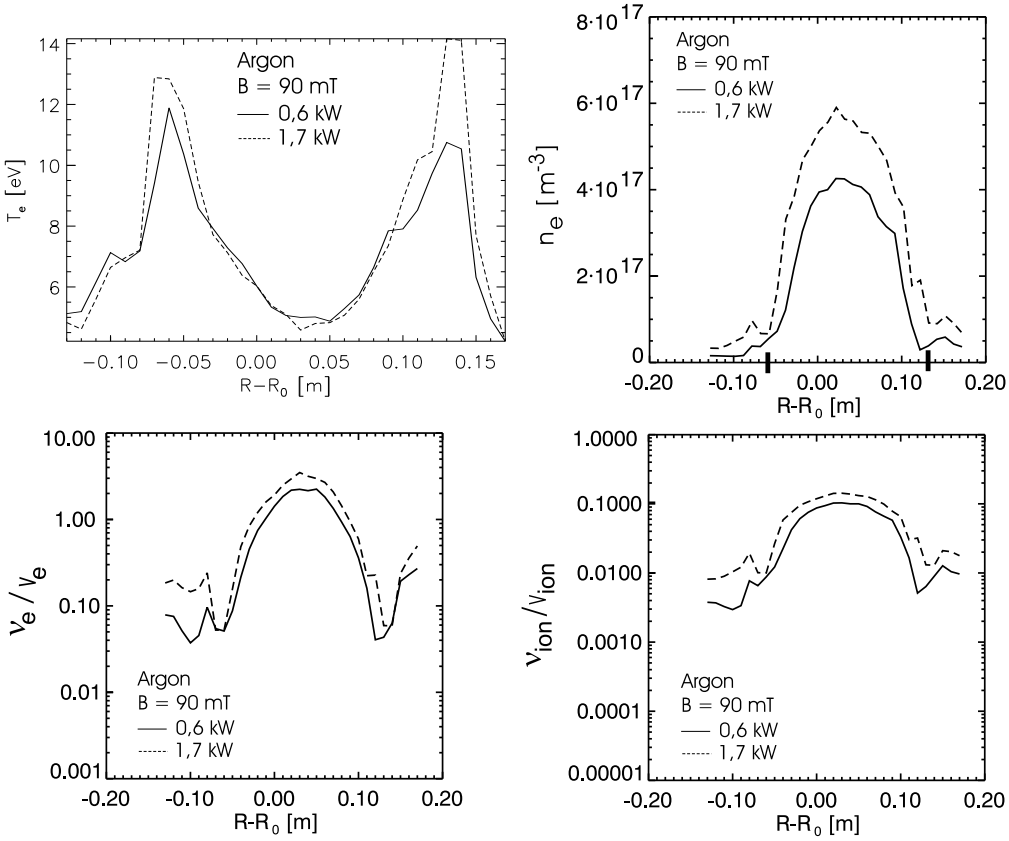

Fig. 4: *Top: Electron temperature and density profiles for an ECRH plasma with Argon ($5 \cdot 10^{-5}$ mbar neutral gas pressure) measured with a Langmuir-Probe. The separatrix, calculated with the Gourdon-Code, is indicated by the black bars in the density plot. Bottom: Collisionalities for electrons and ions. Both are in the Pfirsch-Schlüter regime.*

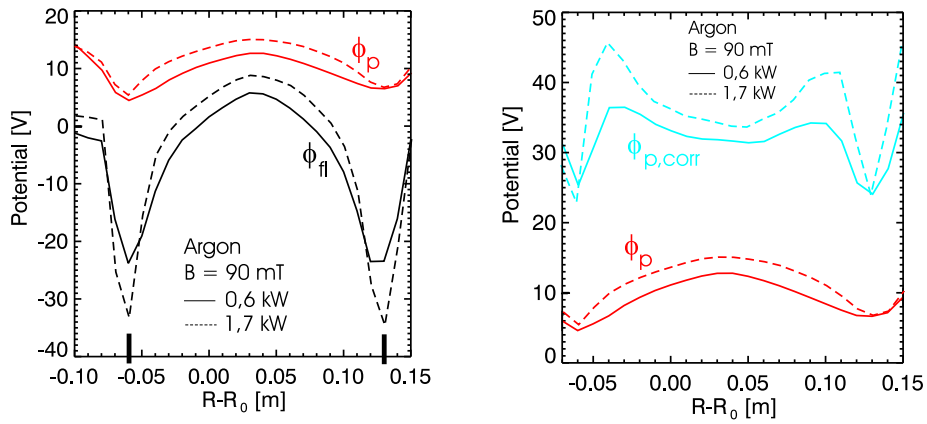

Fig. 5: *In plasma potential the separatrix is not so good pronounced as in floating potential. The corrected plasma potential is much higher than the direct measured one, maybe because of two electron temperatures at the outer radii.*

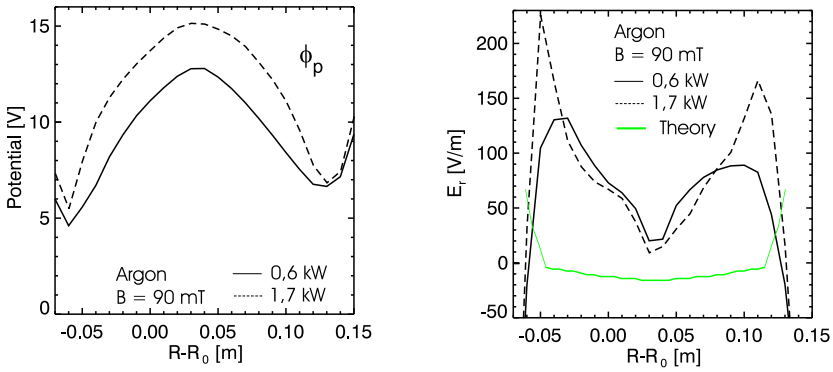

Fig. 6: *Radial electric field getting from an emissive probe direct measured plasma potential in comparison with the theoretical field for the same plasma parameters.*

densities for an ECRH plasma are depicted. They were obtained from Langmuir probe characteristics. Significant is the hollow temperature profile for ECRH discharges at TJ-K. One possible explanation for this phenomenon is, that a large fraction of ECRH power couples at the outer region of the plasma. The density and pressure profile, however, are centrally peaked. In the lower part the collisionality given as ν/v_{th} is depicted, which can directly be compared with Fig. 2. Both electrons and ions are in the Pfirsch-Schlüter regime. In discharges with Helium or Hydrogen lower collisionalities are expected.

From the electron temperature and the floating potential ϕ_{fl}, also obtained from Langmuir probe characteristics, the plasma potential $\phi_{p,corr}$ can be calculated by

$$\phi_{fl} = \phi_{p,corr} + \frac{T_e}{e} \ln\left(0.61\sqrt{2\pi\frac{m_e}{m_i}}\right) . \tag{7}$$

m_e, m_i are electron and ion masses. With emissive probes, a direct measurement of the plasma potential is possible. These probes are, on the other hand, more difficult to handle. For Argon and two heating powers a comparison of different estimates of the plasma potential and is shown in Fig. 5. The floating potential clearly shows a shear layer at the separatrix. In the plasma potential it is also visible, but much less pronounced. As shown on the right, there is no good agreement between the corrected plasma potential $\phi_{p,corr}$ and the one which is directly measured with emissive probes ϕ_p. A possible explanation for this difference is the fact that for the outer radii two electron temperature components may appear. This leads to problems in fitting the Langmuir probe characteristics. The result is a wrong temperature for the correction of the floating potential.

For this reason we rely on the plasma potentials from the direct measurements with emissive probes for comparison with theory. This seems to be a robust method and it is reproducible over a wide range of plasma parameters. Fig. 6 shows the plasma potential and the radial electric field for a selected section. The field is positive in this discharge with values yet to 100 V/m. The theoretical field has only values of -10 V/m in the plasma center. To clarify this difference some theoretical aspects must be discussed. First the toroidal resonance is neglected in the model. Preliminary studies with a simple Ansatz indicate, that it might have an influence on the radial electric field in Argon-plasma. And Second direct electron losses due to the huge helical ripple are not taken into account. In the future, the analysis will be extracted to experiments with Hydrogen and Helium with the objective to rear discharges in the low-collisionality regime.

[1] Shaing, K. C. et al., Proc. 10^{th} Int. IAEA Conf., London, 2(1985), p. 189
[2] Krause, N. et al., Rev. Sci. Instr., **73** (10), 2002, p. 3474
[3] Ascasibar, E. et al., Proc. 15^{th} Int. IAEA Conf., Seville, 1994, p. 749
[4] Beidler, C. D. and Maaßberg, Plasma Phys. Contr. Fusion, **43**(2001), p. 1131.
[5] Maaßberg, H. et al., Phys. Fluids B, **5**(1993), p. 3627
[6] Kadomtsev, B. B. et al., Nuclear Fusion, **11**(1971), p. 67.
[7] Hirshman, S. P. et al., Phys. Fluids, **29** (9), 1986, p. 2151